SARS-CoV-2 infection in the central nervous system of a 1-year-old infant submitted to complete autopsy

Ismael Gomes [1,3]*, Karina Karmirian [2,3]*, Júlia T. Oliveira [2]*, Carolina da S. G. Pedrosa [2]*, Fernando Colonna Rosman [1,5], Leila Chimelli [4#], Stevens Rehen [2,3#]

*These authors contributed equally to this work

#Co-senior authorship

Corresponding author:
Stevens Rehen (srehen@lance-ufrj.org)
+55 21 38836000

Affiliation details:

1 - Anatomic Pathology Service, Jesus Municipal Hospital, Rio de Janeiro, RJ, Brazil.
2 – D'Or Institute for Research and Education (IDOR), Rio de Janeiro, Brazil.
3 – Institute of Biomedical Sciences, Federal University of Rio de Janeiro (UFRJ), Rio de Janeiro, Brazil.
4 - Laboratory of Neuropathology, State Institute of Brain Paulo Niemeyer, Post-Graduate Programs of Pathology and Translational Neuroscience, UFRJ, Rio de Janeiro, RJ, Brazil.
5 - Department of Pathology, School of Medicine, UFRJ, Rio de Janeiro, Brazil.

Abstract

Coronavirus disease 2019 (COVID-19) was initially characterized as a respiratory illness. Neurological manifestations were reported mostly in severely affected patients. Routes for neuroinvasion and the presence of virus particles *in situ* have not been well described, raising controversies about how the virus causes neurological symptoms. Here we report the autopsy findings of a 1-year-old infant with COVID-19. In addition to pneumonitis, meningitis, and multiple organ damage related to thrombosis, a previous encephalopathy may have contributed to the bad clinical outcome. Neuropathological analysis revealed severe cerebral atrophy, cortical nerve cell loss, extensive reactive gliosis, and mild lymphocytic infiltration in the leptomeninges. SARS-CoV-2 infected the choroid plexus, ventricle surfaces, and cerebral cortex. The predominant infection in the choroid plexus along with discontinuous endothelium suggest that neuroinvasion occurred through hematogenous route, due to blood–cerebrospinal fluid barrier disruption. This is the first evidence of SARS-CoV-2 detection and its route of entry in an infant *post-mortem* brain.

Keywords: COVID-19; Choroid Plexus; Neuropathology; Blood–CSF barrier; SARS-CoV-2 neuroinvasion.

Introduction

COVID-19 is caused by Severe Acute Respiratory Syndrome Coronavirus 2 (SARS-CoV-2). Emerged in Wuhan, China, in December 2019, the virus speedily spread globally and has infected more than 34 million people, causing 1,016,000 deaths until late September 2020 (27), with about 35,000 new cases per day worldwide (27), SARS-CoV-2 poses a threat to health systems, especially in countries where the spread of virus was still not mitigated.

COVID-19 is mainly characterized by respiratory signs and symptoms, although severely affected patients can develop acute and chronic neurological symptoms, like headache, dizziness, hypogeusia and hyposmia (12), and clinical impairments, such as persistent fatigue (15) and meningitis/encephalitis (16).

Neurotropism seems to be one of the characteristics of the coronavirus family. Brain samples of a patient that developed SARS presented particles of SARS-CoV, besides an extensive neuronal necrosis and glial hyperplasia (28). Recently, SARS-CoV-2 RNA and proteins were found in the olfactory bulb, superior frontal gyrus, basal ganglia, upper and brainstem, and cerebellum of 53% of patients who died from COVID-19 (13). Another study showed that brain sections of 18 patients presented low levels of SARS-CoV-2 RNA only in 3 sections from the medulla and 3 from the frontal lobe/olfactory nerves of 5 patients (22). Microscopic examination of these samples revealed loss of neurons in the cerebral cortex, hippocampus, and cerebellum (22). The SARS-CoV-2 RNA had also already been reported in cerebrospinal fluid (CSF) of one patient with viral encephalitis (16). However, the route of entry of SARS-CoV-2 into the central nervous system has not been clarified yet.

Here we describe the pathological alterations associated with the presence of SARS-CoV-2 in *post-mortem* tissues of a 1-year and 2-months-old infant, who died from respiratory failure caused by COVID-19. The findings suggest blood-CSF barrier disruption as a via for SARS-CoV-2 entry into the central nervous system.

Case Report

A female infant born in February 2019, at term, healthy, and with normal neurological development, was admitted to an emergency hospital in December 2019 presenting vomits, hypotonia, and seizures. She was discharged after 16 days presenting sporadic episodes of convulsive seizures. Since February 2020, she has been hospitalized three times with seizures and vomits. An electroencephalogram in mid March was abnormal with diffuse slow activity. In early April she was readmitted to the hospital presenting vomits and repetitive movements in the left upper and lower limbs, hypotonia, postural

instability, and inability to support her head, to sit and walk. The auscultation of the respiratory system revealed universally audible vesicular murmur, wheezing, rhonchi, and rales. She evolved with intermittent periods of dyspnea, tachypnea, and use of accessory muscles to breathe, along with tachycardia and fever, anemia, leukocytosis, and relative lymphopenia and neutrophilia. She also presented elevated alanine aminotransferase, aspartate aminotransferase and C-reactive protein, normal bilirubin, and metabolic acidosis and respiratory alkalosis, requiring oxygen therapy and assisted ventilation. The tracheal secretion tested positive for SARS-CoV-2 by RT-PCR, and the cranial computed tomography showed brain atrophy with compensatory hydrocephalus. She evolved to impaired consciousness (Glasgow scale 3), hemodynamic instability, and died twenty-five days after admission, due to respiratory failure caused by bilateral coronavirus pneumonitis.

Materials and Methods

Autopsy procedures and tissue processing

Full autopsy was performed with a *post-mortem* interval of 48 hours and following best practices autopsy guidelines, according to biosafety practices in Anatomical Pathology Laboratories. All tissues were fixed at 10% buffered formalin (pH 7.4) for at least 48 hours.

Tissue samples were processed using a standard protocol for paraffin embedding and 4-µm sections were stained with Hematoxylin and Eosin (H&E). 10-µm sections of selected areas were stained for myelin with Luxol fast Blue. Immunohistochemistry was performed in selected areas of the nervous tissue which presented histological lesions, using anti-glial fibrillary acidic protein (GFAP), anti-NeuN, CD3, CD20, CD34 and CD68 antibodies, according to routine procedures with further detection by DAB-peroxidase system.

For immunofluorescence and confocal imaging, paraffin blocks from lungs and brain (choroid plexus [ChP], cerebral cortex, the surface of lateral ventricle, medulla oblongata, midbrain, pons and putamen) were selected to produce a tissue microarray block, adapted from Pires et al. (20). Then, 4 µm sections were obtained and incubated with anti-SARS-CoV-2 spike protein monoclonal antibody (SP), convalescent serum from a patient with COVID-19 (CS), and double-stranded RNA (dsRNA) monoclonal antibody (J2) overnight at 4°C, followed by Goat anti-Mouse Alexa Fluor 488 secondary antibody incubation. Nuclei were stained with 0.5 µg/mL 4′-6-diamino-2-phenylindole. The images were acquired with a confocal microscope Leica TCS SP8 using a 63x objective lens.

Further details of materials and methods are described in the Supplementary Appendix.

The research protocol was approved at the local Ethics Committee (Copa D'Or Hospital/Instituto D'Or de Pesquisa e Ensino, IDOR, CAAE number: 37211220.0.0000.5249), and was performed according to the Declaration of Helsinki.

Results

Morphological findings

Macroscopic and histopathological examination revealed damages in multiple organs. As expected, coronavirus pneumonitis caused lung congestion and edema (**Figs. 1a, b**); the interstitial inflammation delineated the pulmonary acini (**Fig. 1b**). Histologically, it was characterized by some bronchial lymphoid aggregates, interstitial lymphocytic infiltrate, and diffuse damage of respiratory bronchioles covered with hyaline membranes, along with collapsed alveolar space, some of them containing eosinophilic plugs of plasma proteins and cellular debris (**Fig. 1c, d**). In addition, there was congestion, edema, hemorrhagic foci, atelectasis, and recent microthrombi in some branches of pulmonary arteries in both lungs (**Supp Fig. 1a**).

Other findings included venous and arterial microthrombosis in multiple organs, including small arteries in the lungs, kidneys and left ventricular myocardium (**Supp Figs. 1a-c**). Venous thrombosis was pronounced in vascular structures related to thymus, esophagus, liver and thyroid (**Supp Figs. 1d-g**). We also observed a focal pelvic thrombophlebitis (**Supp Fig. 1h**) and a massive pancreatic ischemic necrosis secondary to vessel thrombosis, along with extensive hemorrhage (**Supp Fig. 1i**) without pancreatitis.

We also found other tissue injuries such as esophagitis and tracheitis, with lymphocyte inflammatory infiltrate in the mucosa (**Supp Figs. 2a-b**), laryngitis with necrosis and mucosal erosion, and hepatic steatosis (**Supp Figs. 2c-d**). Morphological findings are summarized in **Supp Table 1**.

Neuropathological findings

A comprehensive analysis of the encephalic tissues showed severe cerebral atrophy and consequent large remaining space within the cranial cavity (**Fig. 2a**). The brain weight (635 grams) was about 33% less than normal parameters (range weight: 940 to 1,010 grams). On sections, significant atrophy affected the cerebral hemispheres, the cortical surfaces were thin, granulated and discolored (**Fig. 2c**) and there were focal cortical depressions corresponding to areas of cortical collapse, particularly in the temporal lobes which were extremely soft (**Fig. 2b**). The olfactory nerves and bulbs were not preserved

because of the cerebral softening. Cerebellum looked normal and in the brainstem the basis pontis was smaller.

Histologically, pronounced damage was detected in many regions of the cerebral cortex, such as laminar cortical necrosis, spongiosis, microvascular proliferation and diffuse cerebral edema (**Figs. 2d and e**). All lobes were involved, although in some areas, particularly in the temporal lobes, pannecrotic cortical lesions featured profound neuronal loss (**Fig. 2f**) with preserved white matter myelination (**Fig. 2g**). Neuron loss was also observed in the basal ganglia and the thalamus. In the hippocampus, shrunken neurons were seen in CA1 (**Fig. 2i**). The cerebellum was relatively well preserved, with occasional red or shrunken Purkinje cells which were fewer in some regions. Descending axons were reduced in the brainstem. In addition, there were few lymphocytes in the leptomeninges (**Fig. 2h**), particularly in the temporal lobes, and focal perivascular and neuronal mineralization. Severe cortical neuron loss was better detected with NeuN immunostaining (**Fig. 3a and b**) with consequent severe reactive gliosis, also involving basal ganglia and the periventricular region (**Fig. 3c-g**) and microglial/macrophagic proliferation (**Fig. 3h and i**). CD68 positive cells of histiocytic lineage were also seen in the leptomeninges (**Fig. 3j**) where the lymphocytes immunostained with CD3.

SARS-CoV-2 detection in the brain and blood-CSF barrier disruption

We analyzed the lung as a positive control and, as expected, SARS-CoV-2 was present in groups of nearby cells detected by dsRNA, CS (data not shown) and SP (**Fig. 4b-d**). Among brain and brainstem areas, we observed a pronounced SARS-CoV-2 infection localized along the ChP epithelium, mainly in the apical cytoplasm (**Fig. 4f-h and Supp Fig. 3).** Considering that ChP extends within each ventricle in the brain, not surprisingly we also detected SARS-CoV-2 positive cells, to a lesser extent, in the ependyma of the lateral ventricle (**Supp Fig. 3b-d**). We also observed scarce cells positive for SP in the cortex (**Fig. 4j-l**), whereas no positive cells were found in medulla oblongata, pons, midbrain, and putamen (**Supp Fig. 3e-h**).

Interestingly, we also found SARS-CoV-2 infection restricted at the lumina of some choroid plexus capillaries and vessels. This infection pattern was detected by dsRNA (**Fig. 5a-c**), CS (**Fig. 5d-f**), and SP (**Fig. 5g-i**), strongly supporting the presence of the virus in those areas. Furthermore, other vessels showed the entire wall infected by SARS-CoV-2 (**Supp Fig. 4e and f**). Notably, the group of cells localized nearby the infected endothelium presented higher immunoreactivity to SARS-CoV-2 than other cells alongside the vessels (**Fig. 5a and c, Supp Fig. 4b, c and e**), suggesting the course of viral infection and its spread. As we found substantially SARS-CoV-2 positive staining in the epithelium and endothelium of the ChP, we investigated the integrity of ChP endothelium. The staining for the

endothelial marker CD34 showed a discontinuity in multiple sites of the vessels of ChP, probably as a result of SARS-CoV-2 infection (**Fig. 6**).
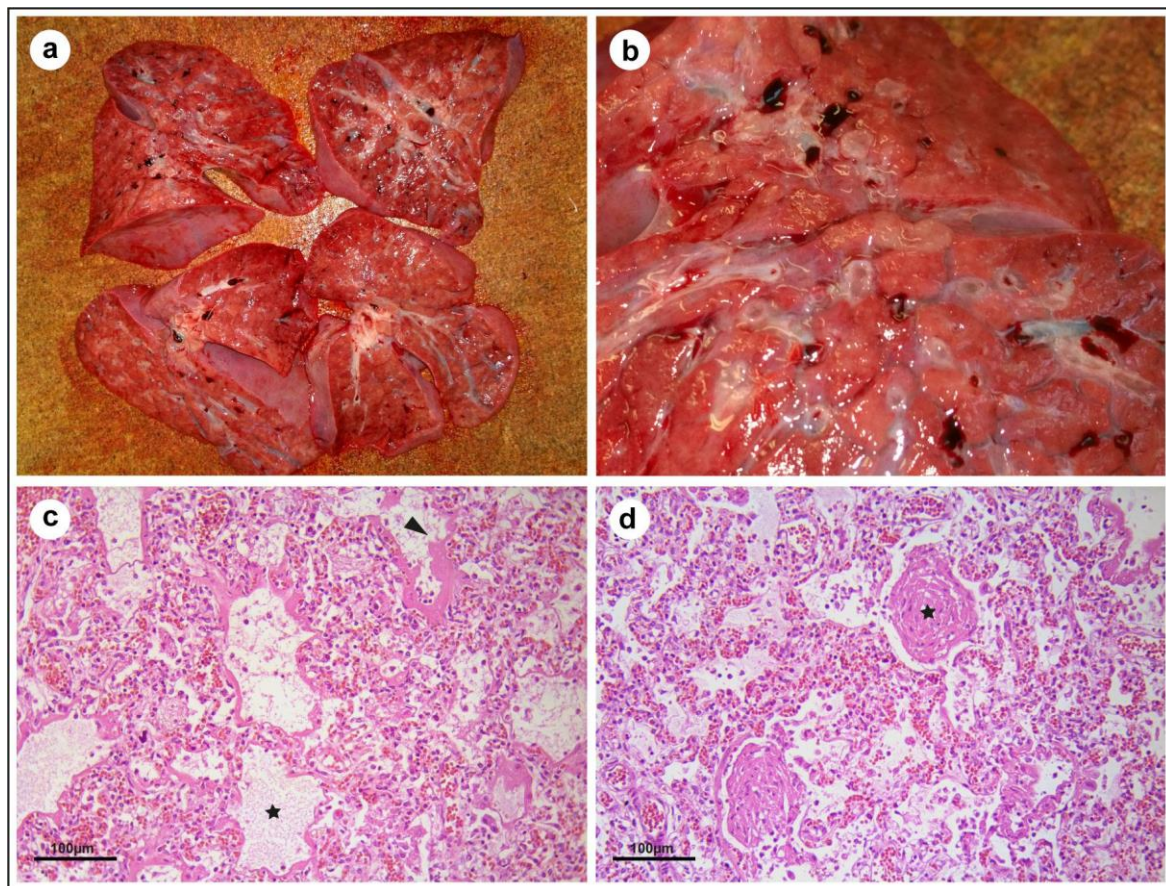
Fig. 1 Macroscopic and microscopic appearances of lungs
(a) Cut surfaces of the left (above) and the right (below) congested and edematous lungs. In (b) the pulmonary acini (lobules) are well delimited due to the pneumonitis. *Post-mortem* clots are seen in branches of pulmonary arteries. (c) Diffuse damage of respiratory bronchioles (star), associated with eosinophilic hyaline membranes (arrowhead). Note the congestion of the alveolar capillaries, the collapsed alveolar spaces and the interstitial lymphocytic infiltrate. (d) Respiratory bronchioles with eosinophilic plugs (star) of plasma proteins and cellular debris. Observe the collapsed alveolar spaces and some hyaline membranes. (c and d - H&E).
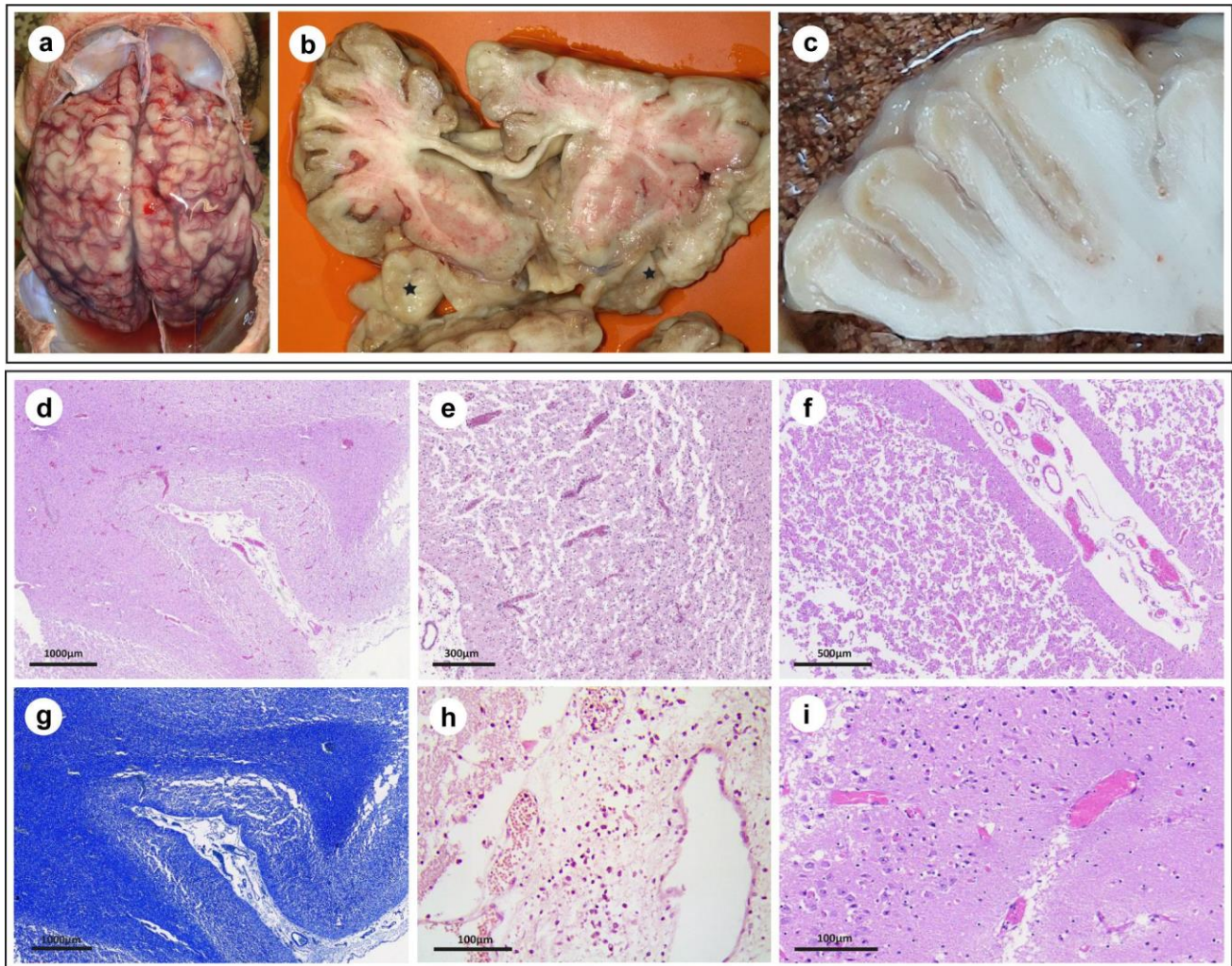
Fig. 2 Macroscopic and microscopic appearances of brain tissue
(a) Unfixed brain *in situ* does not fill the base of the skull due to marked atrophy. **(b)** Coronal section of the brain with cortical atrophy and wide sulci. The flat cortical surface of the right hemisphere is due both to edema and fixation artifacts. The temporal lobes (stars) have collapsed due to cortical necrosis, as seen histologically in **(f)**. **(c)** Cut surface of fixed brain showing thin granular and discolored cortex. **(d)** Histological section of cortex and white matter, showing cortical laminar necrosis. Detail in **(e)**. There is severe nerve cell loss and vascular proliferation, but the molecular layer (left) is relatively spared. **(g)** White matter myelination is preserved as seen with the Luxol Fast Blue staining. **(h)** Mild lymphocytic infiltration is seen in the leptomeninges. In **(i)**, CA1 hippocampal neurons (mid-upper right) although present, are shrunken compared to those in CA2 (lower left).(**d-f** and **h-i** - H&E).
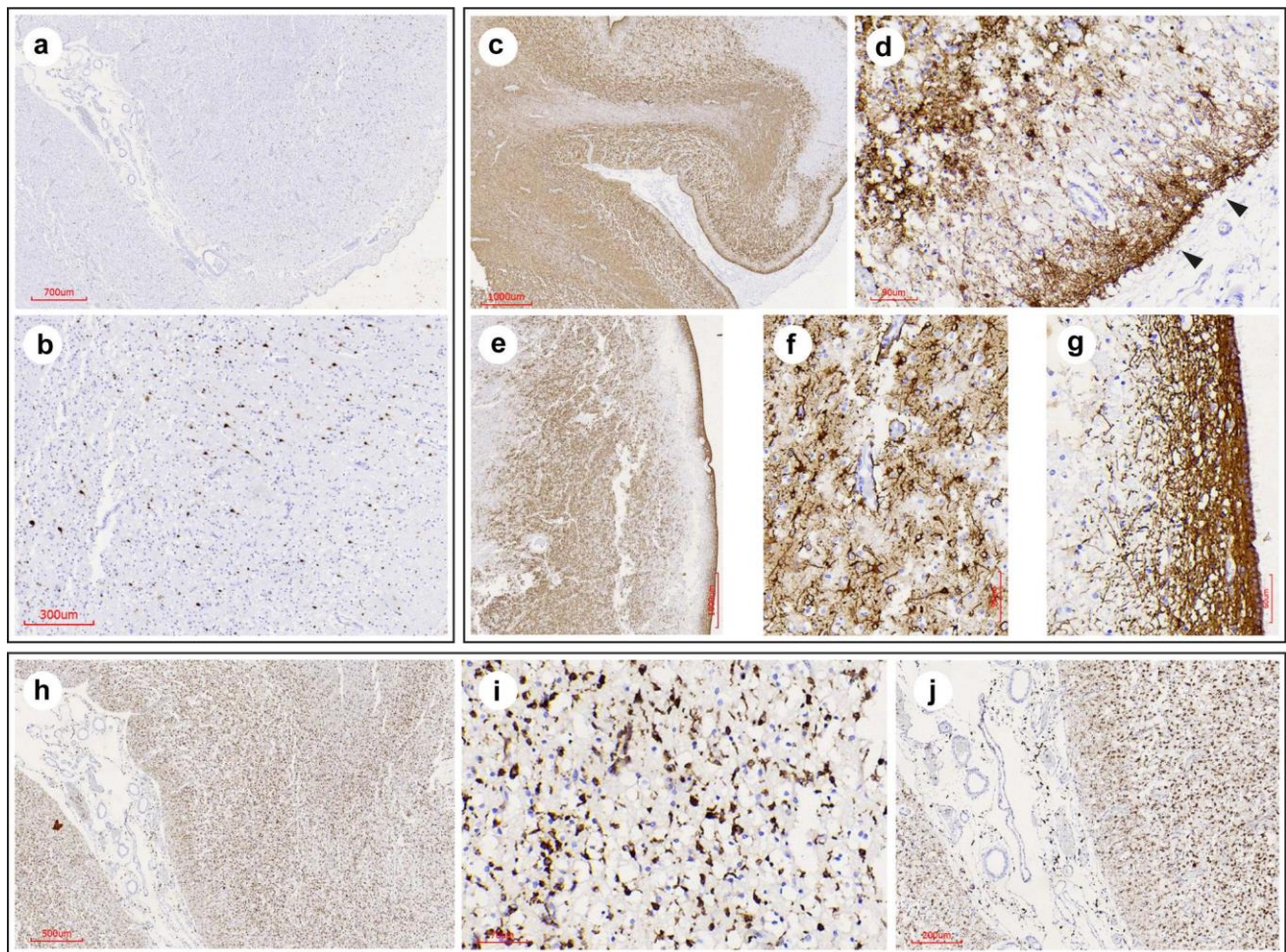
Fig. 3 Immunostainings with NeuN (a-b), GFAP (c-g) and CD68 (h-j) in cerebral areas

Severe cortical nerve cell loss **(a)** compared with a transition with a better-preserved area **(b)**, where scattered pyramidal neurons are present. **(c)** Severe reactive gliosis involving cortex and white matter, except in an area where the cortical nerve cell and axonal loss (in the corresponding white matter) was not so severe (upper right corner). A detail of the cortical gliosis is seen in **(d)**, including the subpial region (arrowheads), sparing part of the molecular layer. **(e)** Caudate nucleus and periventricular region, including the ependymal surface with severe gliosis. Details in **(f)** and **(g)**, respectively. **(h)** Microglial and macrophagic proliferation in cortex and white matter (detail in **i**). In **(j)** a detail of CD68 positive cells of histiocytic lineage in the leptomeninges.
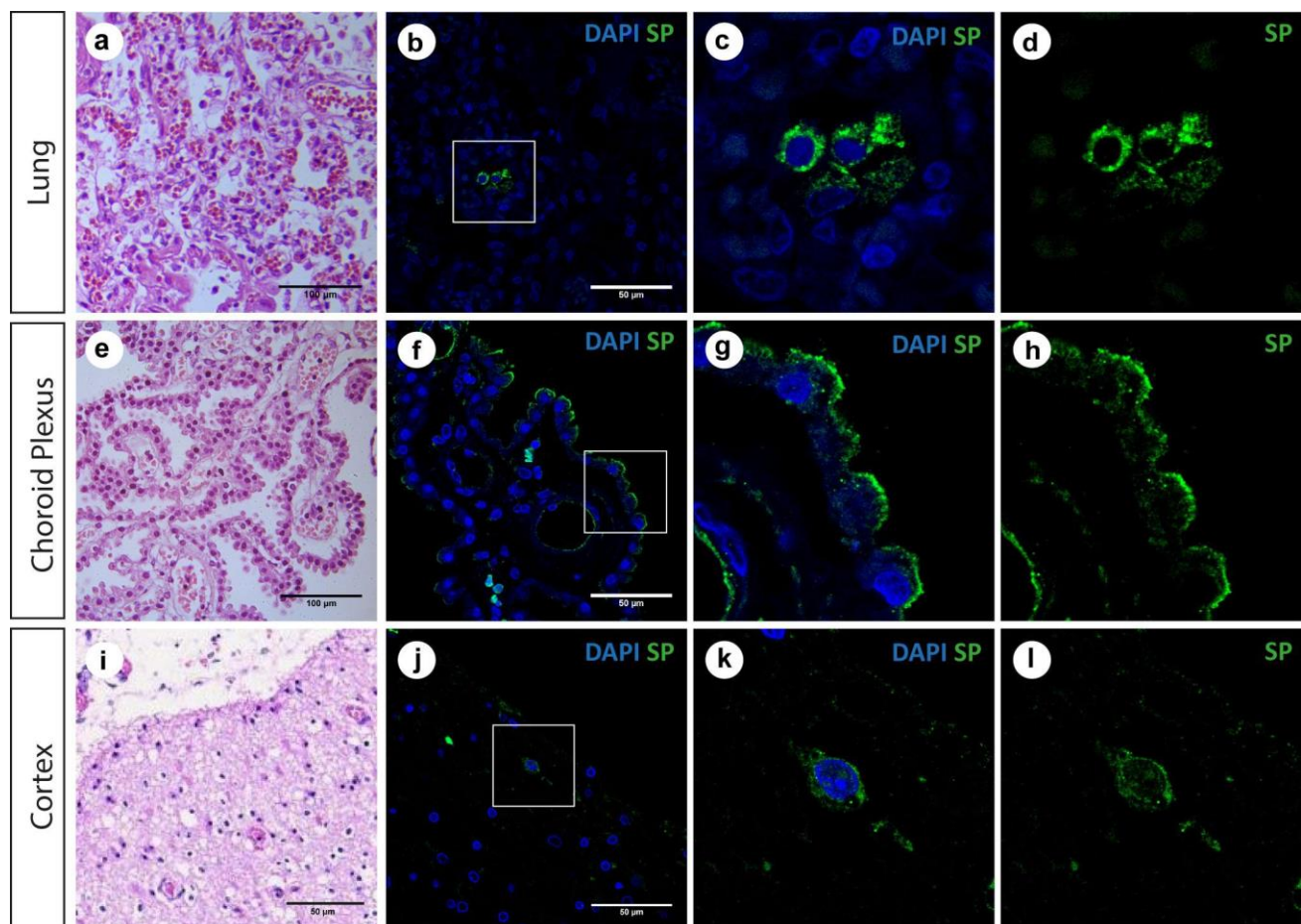
Fig. 4 Light and immunofluorescence staining photomicrographs for spike protein (SP) in the brain (cerebral cortex and choroid plexus) and lung

(a) Lung tissue with marked pneumonitis. (b-d) SARS-CoV-2 infected cells in the lung detected by SP (green) and nuclear staining in blue (DAPI). (e) Choroid plexus of the cerebral lateral ventricle. Note vascularized and ramified papillary structures covered with a simple cuboidal epithelium. (f-h) SARS-CoV-2 infected cells in the choroid plexus detected by SP. (i) Molecular layer of cerebral cortex. (j-l) SARS-CoV-2 infected cells detected in the cortex by SP. (a, e, i - H&E).
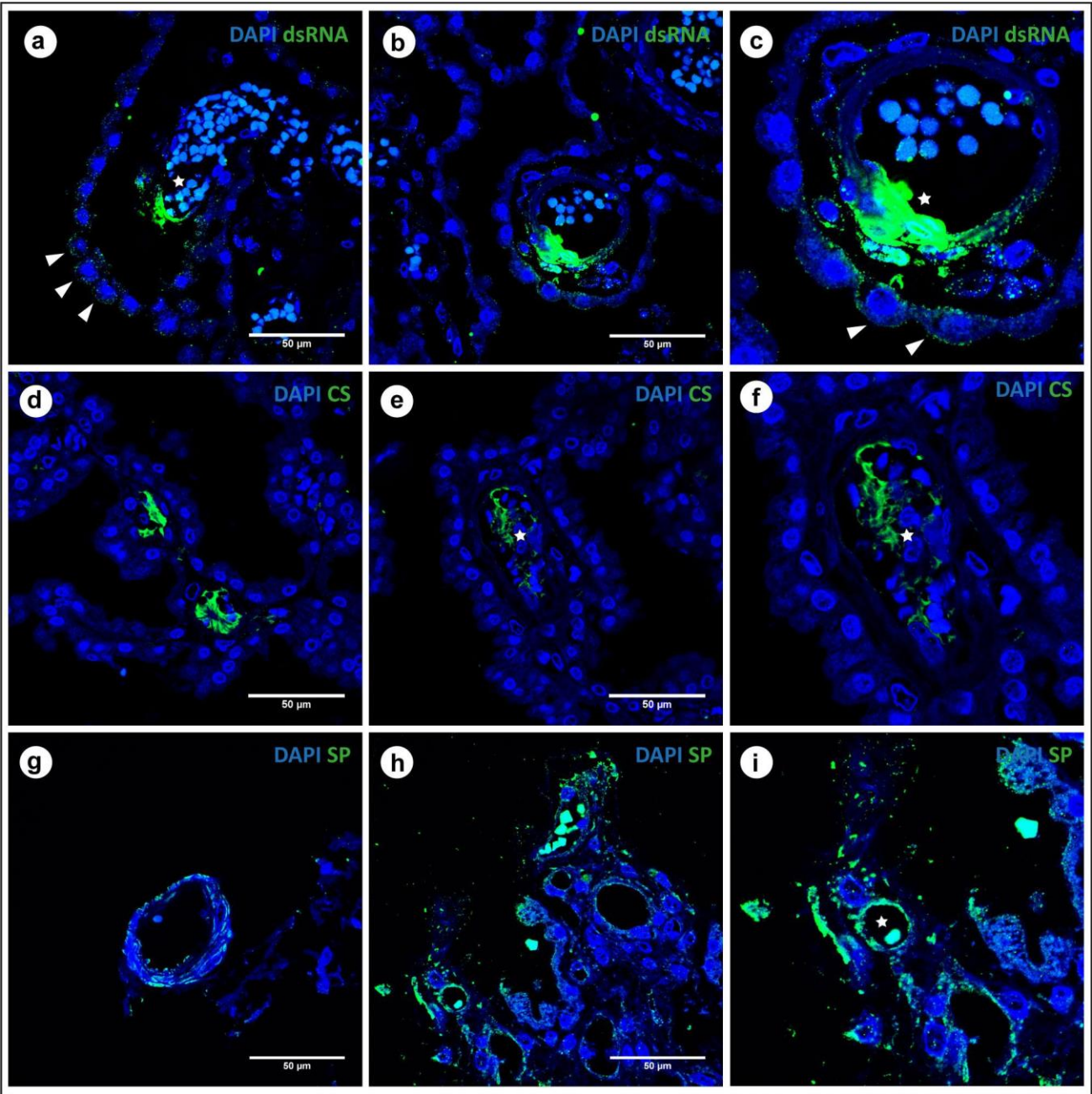
Fig. 5 Immunofluorescence photomicrographs for SARS-CoV-2 in the choroid plexus endothelium. Immunostaining for dsRNA (a-c), CS (d-f) and spike protein (SP) (g-i) in green and nuclear staining in blue (DAPI). SARS-CoV-2 infection at the lumina of capillaries and vessels (stars) and nearby cells infected (arrowheads). Details in (c), (f) and (i).
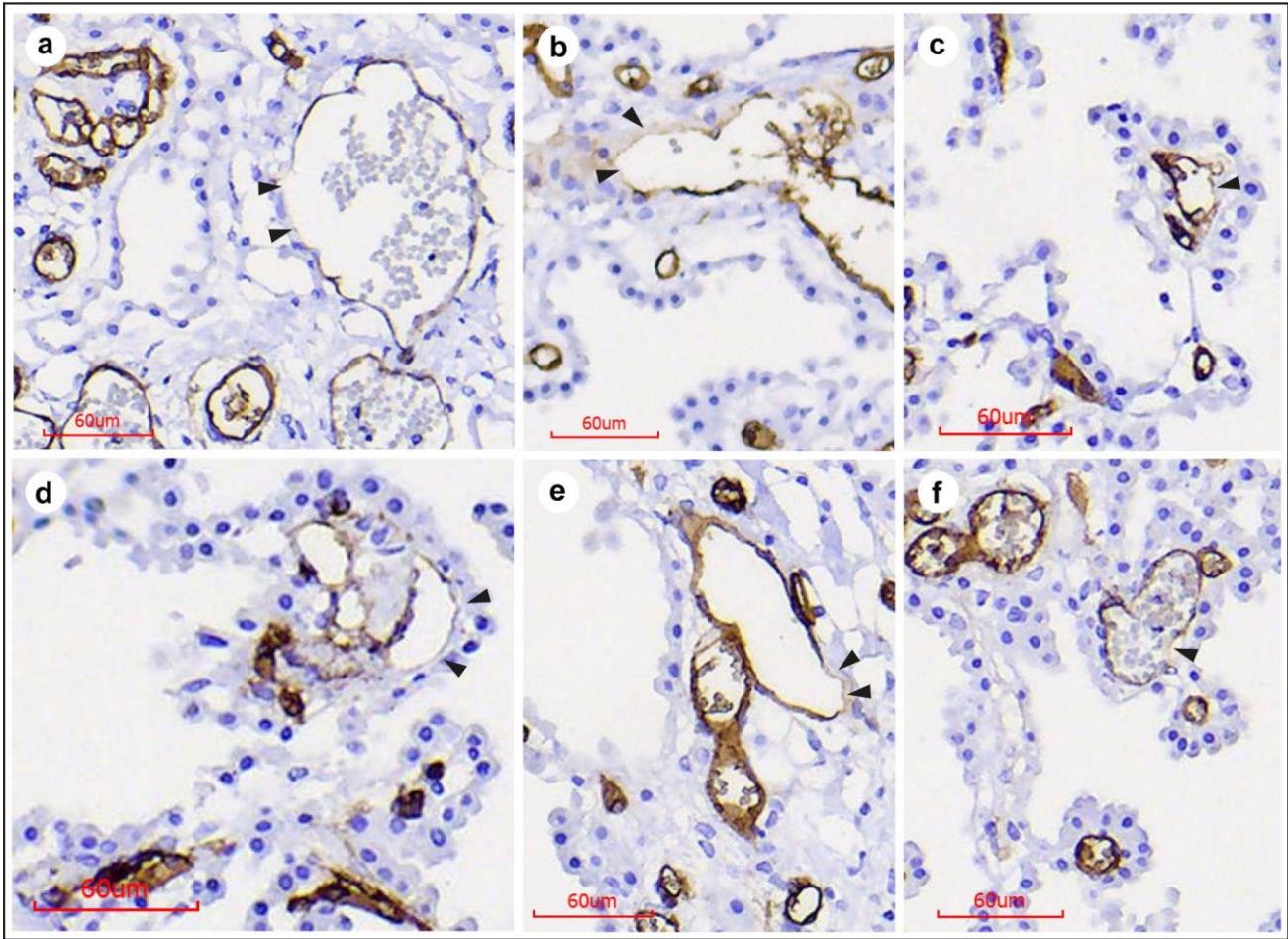
Fig. 6 CD34 immunoreaction for endothelial cells in the choroid plexus. (a-f)
CD34 is discontinuous or weakly stained (arrowheads) in several regions of the choroid plexus vessel walls.

Discussion

We reported the histopathological *post-mortem* findings of a 1-year and 2-months-old infant that died of COVID-19. We observed a severe pneumonitis and a massive cerebral hypotrophy and edema with morphological appearances of hypoxic encephalopathy (a co-morbidity that might have contributed to the bad outcome of COVID-19), secondary to the prolonged episodes of seizures and the respiratory disease. We also demonstrated that SARS-CoV-2 substantially infected the choroid plexus epithelium and endothelium, some ependymal cells and in a lesser extension the cerebral cortex.

The cause of death was a severe pneumonitis with diffuse respiratory bronchiolar and alveolar damage, together with massive pancreatic ischemic necrosis secondary to a large vessel thrombosis, both reported in patients infected with the SARS-CoV-2 (5,4). In addition, the infant presented multiple thrombotic events in several organs. *Post-mortem* studies have shown microangiopathy and microthrombosis in major organs, including the lungs (5,2).

Another hallmark of severe COVID-19 is the overproduction of proinflammatory cytokines which leads to systemic inflammation (18) and contributes to thrombus formation (25,10). We observed leukocytes infiltration, hyaline membranes and plugs of plasma proteins and cellular debris in the lung parenchyma, but lymphoid depletion was also detected in lymphoid tissues, as previously reported (5).

The encephalopathy reported here could be related to hypoxia, secondary to both the prolonged episodes of seizures and the severe pneumonitis. However, a differential diagnosis with Alpers-Huttenlocher syndrome (which has morphological features of anoxic encephalopathy and liver steatosis), cannot be ruled out (21). It was not suspected in life, there was no family history and unfortunately molecular genetic diagnosis is not available, but could explain the clinical presentation, from the first symptoms. On the other hand, other causes of liver steatosis such as antiepileptic drugs, steroids, taken by this child, and even under nutrition due to the various episodes of vomits in the last few months, should also be taken into account. Together with severe cortical neuron loss, reactive gliosis is expected in both encephalopathies, particularly in the cortex, as well as macrophagic activity. However, excessive microgliosis and white matter gliosis was unexpected and could be related to SARS-CoV-2 infection. In fact, it has been reported increased plasma levels of GFAP and neurofilament light chain protein in COVID-19 severe patients, which might explain the outcomes of cerebral injury related to SARS-CoV-2 infection (9) and the neurological signs and symptoms. Systemic lymphoid depletion (see **Supplementary Table 1**), the use of steroids, and possible late and mild viral invasion, could also explain the fact that leptomeningitis in this case (described for the first

time in children in association with SARS-CoV-2 infection) coursed with mild lymphocytic infiltration.

Despite the suggested neurological infection, the route of SARS-CoV-2 entry into the brain is still under debate. Recently, it was demonstrated infection by SARS-CoV-2 associated with local ischemic infarctions in the adult human brain (23). SARS-CoV-2 uses the angiotensin-converting enzyme 2 (ACE2) as the main entry in the host cells. ACE2 is mainly expressed in the heart, kidney, small intestine, testis, placenta, eye and vessels. The brain presents negligible amounts of ACE2 protein, except for the choroid plexus, which exhibits high expression of ACE2 (6,3). Indeed, we found considerable immunostaining for SARS-CoV-2 in choroid plexus and, to a lesser extent, in ependymal cells, but it was scarce in other brain areas, such as the cortex, probably due to a very mild infection.

Choroid plexus has a single epithelial layer attached by tight junctions that participates in the blood-cerebrospinal fluid (CSF) barrier (11,1,7). A study evidenced SARS-CoV-2 particles in endothelial cells, as well as inflammation (26). Another study found viral-like particles in brain capillary endothelium suggesting the hematogenous route as the most likely pathway for SARS-CoV-2 to the brain (17). Given the essential role of endothelium in vascular permeability homeostasis, endothelium dysfunction caused by SARS-CoV-2 infection may contribute to the thrombo-inflammatory process resulting in vasculopathy (14). Thus, infection of the choroid plexus could enable SARS-CoV-2 to disrupt the CSF barrier and invade the brain and is supported by our finding of discontinuous CD34 staining in choroid plexus endothelial cells.

Our findings are in accordance with previous works *in vitro* showing choroid plexus infection by SARS-CoV-2 in brain organoids (19,8). The authors demonstrated that SARS-CoV-2 has minimal tropism for neurons and glial cells but promotes the brain-CSF barrier breakdown (19). Likely, the deleterious findings in the *post-mortem* brain tissues was due to the previous encephalopathy added to the entry of immune cells and cytokines through the disrupted blood-CSF barrier. Supporting this concept, SARS-CoV-2 RNA was found in the cerebrospinal fluid of one patient with COVID-19 encephalitis, as aforementioned (16).

Here we reported several multisystemic histopathological alterations caused by SARS-CoV-2 in an infant. Severe SARS-CoV-2 cases in children are rare but concerning because they may result in death or sequelae in many cases (24). The differences of SARS-CoV-2 behavior between children and adults are not clear, but they seem to share hallmarks, including inflammation, thrombosis, and secondary tissue hypoxia. Indeed, the histopathological findings showed all these aspects in addition to

meningitis. We also showed the discontinuity of the endothelium and substantially SARS-CoV-2 infection in the choroid plexus *in vivo*. Our findings suggest SARS-CoV-2 neuroinvasion may occur via blood-CSF barrier disruption. Further research is needed to better understand the mechanisms that can trigger blood-CSF barrier disruption. Although SARS-CoV-2 does not diffuse effectively within the brain it might profoundly damage it, since the excessive microgliosis observed in this case was unexpected in the previous encephalopathy. This report elucidates many aspects of SARS-CoV-2 infection contributing to the search for clinical and pharmacological strategies against COVID-19.

Acknowledgements

We thank Leticia Souza for technical support in confocal images acquisition; Diego Santos and Heliomar Pereira Marcos for immunohistochemical staining technique. Financial support (not specifically for COVID-19 studies) was provided by the Foundation for Research Support in the State of Rio de Janeiro (FAPERJ); the National Council of Scientific and Technological Development (CNPq) and Coordination for the Improvement of Higher Education Personnel (CAPES), in addition to intramural grants from D'Or Institute for Research and Education.

Author contributions

Ismael C. Gomes, Fernando Colonna Rosman and Stevens Rehen conceptualized the study. Fernando Colonna Rosman performed the autopsy and full histological analysis. Leila Chimelli performed the neuropathological analysis. Ismael C. Gomes performed material preparation for histological procedures and immunofluorescence stainings. Ismael C. Gomes, Karina Karmirian and Carolina da S. G. Pedrosa performed confocal images analysis. Karina Karmirian and Leila Chimelli prepared the figure panels. The first draft of the manuscript was written by Karina Karmirian, Julia T. Oliveira and Carolina da S. G. Pedrosa. All authors discussed the results and contributed to the final version of the manuscript. All authors read and approved the final manuscript. Leila Chimelli and Stevens Rehen coordinated the study.

Competing interests

The authors declare no competing interests.

References

1. Brightman MW (1968). The Intracerebral Movement of Proteins Injected into Blood and Cerebrospinal Fluid of Mice. Prog Brain Res 29:19-40. https://doi.org/10.1016/S0079-6123(08)64147-3

2. Carsana L, Sonzogni A, Nasr A et al (2020). Pulmonary post-mortem findings in a series of COVID-19 cases from northern Italy: a two-centre descriptive study. Lancet Infect Dis 20(10):1135-1140. https://doi.org/10.1016/S1473-3099(20)30434-5

3. Chen R, Wang K, Yu J, Chen Z, Wen C, Xu Z (2020). The spatial and cell-type distribution of SARS-CoV-2 receptor ACE2 in human and mouse brain. BioRxiv. https://doi.org/10.1101/2020.04.07.030650

4. Duarte-Neto AN, Monteiro RA de A, da Silva LFF et al (2020). Pulmonary and systemic involvement of COVID-19 assessed by ultrasound-guided minimally invasive autopsy. Histopathology. https://doi.org/10.1111/his.14160

5. Hanley B, Naresh KN, Roufosse C et al (2020). Histopathological findings and viral tropism in UK patients with severe fatal COVID-19: a post-mortem study. Lancet Microbe. https://doi.org/10.1016/S2666-5247(20)30115-4

6. Hikmet F, Méar L, Edvinsson Å, Micke P, Uhlén M, Lindskog C (2020). The protein expression profile of ACE 2 in human tissues. Mol Syst Biol 16: e9610. https://doi.org/10.15252/msb.20209610

7. Hilhorat TH, Davis DA, LIoyd BJ Jr (1973). Two morphologically distinct bloodbrain barriers preventing entry of cytochrome C into cerebrospinal fluid. Science 180(4081):76-78. https://doi.org/10.1126/science.180.4081.76

8. Jacob F, Pather SR, Huang WK et al (2020). Human Pluripotent Stem Cell-Derived Neural Cells and Brain Organoids Reveal SARS-CoV-2 Neurotropism. BioRxiv. https://doi.org/10.1101/2020.07.28.225151

9. Kanberg N, Ashton NJ, Andersson LM et al (2020). Neurochemical evidence of astrocytic and neuronal injury commonly found in COVID-19. Neurology 95(12):e1754-e1759. https://doi.org/10.1212/WNL.0000000000010111

10. Lazzaroni MG, Piantoni S, Masneri S et al (2020). Coagulation dysfunction in Covid-19: The interplay between inflammation, viral infection and the coagulation system. Blood Rev 100745. https://doi.org/10.1016/j.blre.2020.100745

11. Lun MP, Monuki ES, Lehtinen MK (2015). Development and functions of the choroid plexus – cerebrospinal fluid system. Nat Rev Neurosci 16(8):445-457. https://doi.org/10.1038/nrn3921

12. Mao L, Jin H, Wang M et al (2020). Neurological Manifestations of Hospitalized Patients With Coronavirus Disease 2019 in Wuhan, China. JAMA Neurol 77(6):638-690. https://doi.org/10.1001/jamaneurol.2020.1127

13. Matschke J, Lütgehetmann M, Hagel C et al (2020). Neuropathology of patients with COVID-19 in Germany: a post-mortem case series. Lancet Neurol. Epub ahead of print. https://doi.org/10.1016/S1474-4422(20)30308-2

14. Mcgonagle D, Donnell JSO, Sharif K, Emery P, Bridgewood C (2020). Immune mechanisms of pulmonary intravascular coagulopathy in COVID-19 pneumonia. Lancet Rheumatol 2(7):e437-e445. https://doi.org/10.1016/S2665-9913(20)30121-1

15. Montalvan V, Lee J, Bueso T, De Toledo J, Rivas K (2020). Neurological manifestation of COVID-19 and other coronavirus infections: A systematic review. Clin Neurol Neurosurg 194:105921. https://doi.org/10.1016/j.clineuro.2020.105921

16. Moriguchi T, Harii N, Goto J et al (2020). A first case of meningitis/encephalitis associated with SARS-Coronavirus-2. Int J Infect Dis 94:55–58. https://doi.org/10.1016/j.ijid.2020.03.062

17. Paniz-Mondolfi A, Bryce C, Grimes Z et al (2020). Central nervous system involvement by severe acute respiratory syndrome coronavirus-2 (SARS-CoV-2). J Med Virol(92):699–702. https://doi.org/10.1002/jmv.25915

18. Pedersen SF, Ho YC (2020). SARS-Cov-2: a storm is raging. J Clin Invest 130(5):2202-2205. https://doi.org/10.1172/JCI137647

19. Pellegrini L, Albecka A, Mallery DL et al (2020). SARS-Cov-2 infects brain choroid plexus and disrupts the blood-CSF-barrier. BioRxiv. https://doi.org/10.1101/2020.08.20.259937

20. Pires ARC, Andreiuolo F da M, de Souza SR (2006). TMA for all : a new method for the construction of tissue microarrays without recipient paraffin block using custom-built needles. Diagn Pathol 1:14. https://doi.org/10.1186/1746-1596-1-14

21. Simonati A, Filosto M, Savio C et al (2003). Features of cell death in brain and liver, the target tissues of progressive neuronal degeneration of childhood with liver disease (Alpers-Huttenlocher disease). Acta Neuropathol 106(1):57-65. https://doi.org/10.1007/s00401-003-0698-x

22. Solomon IH, Normandin E, Bhattacharyya S et al (2020). Neuropathological Features of Covid-19. N Engl J Med. 383(10):989-992. https://doi.org/10.1056/NEJMc2019373

23. Song E, Zhang C, Israelow B et al (2020). Neuroinvasion of SARS-CoV-2 in human and mouse brain. BioRxiv. https://doi.org/10.1101/2020.06.25.169946

24. Stafstrom CE, Jantzie LL (2020). COVID-19: Neurological Considerations in Neonates and Children. Children 7(9):133. https://doi.org/10.3390/children7090133

25. Tufan A, Avanoğlu Güler A, Matucci-Cerinic M (2020). COVID-19, immune system response, hyperinflammation and repurposing antirheumatic drugs. Turk J Med Sci 50(SI-1):620-632. https://doi.org/10.3906/sag-2004-168

26. Varga Z, Flammer AJ, Steiger P et al (2020). Endothelial cell infection and endothelitis in

COVID-19. Lancet 395(10234):1417-1418. https://doi.org/10.1016/S0140-6736(20)30937-5

27.   Worldometer (2020). Reported coronavirus Cases. In: COVID-19 Coronavirus Pandemic. Available from: https://www.worldometers.info/coronavirus. Accessed 30 Sep 2020.

28.   Xu J, Zhong S, Liu J et al (2005). Detection of Severe Acute Respiratory Syndrome Coronavirus in the Brain : Potential Role of the Chemokine Mig in Pathogenesis. Clin Infect Dis 41(8):1089–1096. https://doi.org/10.1086/444461